

First directional European palaeosecular variation curve for the Neolithic based on archaeomagnetic data

Á. Carrancho^{a,*}, J.J. Villalaín^b, F.J. Pavón-Carrasco^{c,d}, M.L. Osete^{d,e}, L.G. Straus^{f,k}, J.M. Vergès^{g,h}, J.M. Carreteroⁱ, D.E. Angelucci^j, M.R. González Morales^k, J.L. Arsuaga^{l,m}, J.M. Bermúdez de Castroⁿ, E. Carbonell^g

^a Área de Prehistoria, Dept. Ciencias Históricas y Geografía, Universidad de Burgos, Edificio I+D+I, Plaza Misael Bañuelos s/n, 09001 Burgos, Spain
^b Dpto. Física, Universidad de Burgos, Escuela Politécnica Superior, Avda. Cantabria s/n, 09006 Burgos, Spain
^c Istituto Nazionale di Geofisica e Vulcanologia, Sezione Roma 2, Via di Vigna Murata, 605, 00143 Roma, Italy
^d Dept. Física de la Tierra I, Facultad de Ciencias Físicas, Universidad Complutense, 28040 Madrid, Spain
^e Instituto de Geociencias (IGEO) CSIC, UCM, Ciudad Universitaria, 28040 Madrid, Spain
^f Dept. of Anthropology MSC01 1040, University of New Mexico, Albuquerque, NM 87131-0001, USA
^g IPHES, Institut Català de Paleoecologia Humana i Evolució Social, C/Marcel·lí Domingo s/n, Campus Sescelades (Edifici W3), 43007 Tarragona, Spain
^h Área de Prehistoria, Universitat Rovira i Virgili (URV), Avinguda de Catalunya, 35, 43002 Tarragona, Spain
ⁱ Laboratorio de Evolución Humana, Departamento de Ciencias Históricas y Geografía, Universidad de Burgos, Edificio I+D+I, Plaza de Misael Bañuelos s/n, 09001 Burgos, Spain
^j Dipartimento di Lettere e Filosofia, Università degli Studi di Trento, via T. Gar 14, 38122 Trento, Italy
^k Instituto Internacional de Investigaciones Prehistóricas de Cantabria, Universidad de Cantabria, Avda. de los Castros s/n, 39071 Santander, Spain
^l Centro de Evolución y Comportamiento Humanos (UCM-ISCH), Instituto de Salud Carlos III, C/Monforte de Lemos 5, Pabellón 14, 28029 Madrid, Spain
^m Departamento de Paleontología, Facultad de Ciencias Geológicas, Universidad Complutense de Madrid, 28040 Madrid, Spain
ⁿ National Research Center for Human Evolution (CENIEH), Paseo Sierra de Atapuerca s/n, 09002 Burgos, Spain

ABSTRACT

Neolithic, Chalcolithic and Bronze Age anthropogenic cave sediments from three caves from northern Spain have been palaeomagnetically investigated. 662 oriented specimens corresponding to 39 burning events (ash–carbonaceous couplets) from the three sites with an average of 16 samples per fire were collected. 26 new archaeomagnetic directions have been obtained for the time period ranging from 5500 to 2000 yr cal. BC. These results represent the oldest archaeomagnetic directions obtained from burnt archaeological materials throughout all Western Europe. Magnetisation is carried by pseudo-single domain low-coercivity ferromagnetic minerals (magnetite, magnetite with no significant isomorphous substitution and/or maghaemite). Rock-magnetic experiments indicate a thermoremanent origin of the magnetisation although a thermochemical magnetisation cannot be excluded. Combination of the new data presented here and the recent updated Bulgarian database allows us to propose the first European palaeosecular variation (PSV) curve for the Neolithic. A bootstrap method was applied for the curve construction using penalised cubic B-splines in time. The new palaeosecular variation curve is well constrained from 6000 BC to 3700 BC, the period with the highest density of data, showing a declination maximum around 4700 BC and a minimum in inclination at 4300 BC, which are not recorded by the recent global CALS10K.1b and regional SCHA.DIF.8K models due to the use of lake sediment data. Dating resolution by using the proposed PSV curve oscillates from approximately ± 30 yr to ± 200 yr for the period 6000 to 1000 yr BC, reaching similar resolution as radiocarbon dating. Considering the good preservation, age-control and widespread occurrence of burnt archaeological materials across Southern Europe, they represent a new source of data for geomagnetic field modelling, as well as for archaeomagnetic dating.

Keywords:
secular variation
archaeomagnetism
rock-magnetism
thermoremanence
Neolithic
archaeology

1. Introduction

Knowledge of long-term variation of the Earth's magnetic field (palaeosecular variation) is a forefront research area in Solid Earth Sciences. Determinations of the palaeofield are necessary to expand global and regional geomagnetic field models, whose applications range from the reconstruction of field geometry to

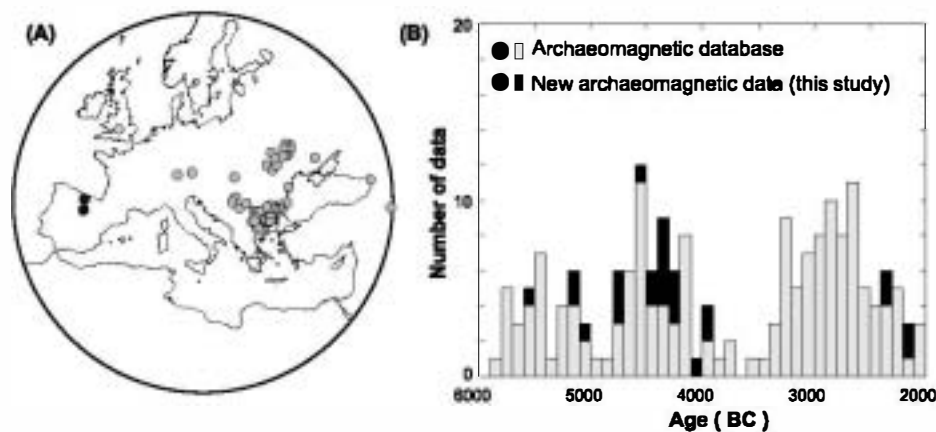


Fig. 1. (A–B) Spatial and temporal distribution of archaeomagnetic directions in Europe (6000–2000 yr BC). Archaeomagnetic database in grey (after Kovacheva et al., 2009; Korte et al., 2011).

archaeomagnetic dating. Reconstruction of geomagnetic field variations prior to instrumental measurements (last few centuries, e.g. Alexandrescu et al., 1997; Jonkers et al., 2003), has been traditionally addressed through the analysis of well-dated magnetised sediments, lavas or archaeological burnt material. Sedimentary sequences provide relatively long and continuous palaeomagnetic records with broad geographical distribution. However, their magnetisation lock-in is delayed, due to the mechanism of remanence acquisition. Moreover, the magnetisation in sedimentary contexts is subjected to several factors that could cause errors in the palaeomagnetic record such as flattening or bioturbation, among others. Consequently, geomagnetic models that incorporate sedimentary data introduce a “smoothing effect” producing low resolution reconstructions of geomagnetic field variations (e.g. Donadini et al., 2009; Korte et al., 2011; Pavón-Carrasco et al., 2010). In contrast, burnt archaeological materials and lava flows usually carry a stable thermoremanence which gives spot information of the palaeofield and are thus considered the best records of the geomagnetic field.

In order to obtain a detailed picture of the geomagnetic field variation, the classical approach is to develop local palaeosecular variation (PSV) curves from well-dated, *in situ* archaeomagnetic materials carrying a thermoremanence. In recent years, new or updated PSV curves have been published in different European regions covering reasonably well the last 2–3 millennia (Gallet et al., 2002; Gómez-Paccard et al., 2006; Hervé et al., 2013; Kovacheva et al., 2009; Márton and Ferencz, 2006; Schnepf and Lanos, 2005, 2006; Tema et al., 2006; Tema and Kondopoulou, 2012; Zananiri et al., 2007). In spite of great advances, at present, very few archaeomagnetic directions are available in Europe before the third millennium BC (Fig. 1A–B). No archaeomagnetic information from Western Europe are provided by the global database, with the only exception of a study in the UK carried out during the 1960s (Aitken and Hawley, 1967) and one direction from the fourth millennium BC from France (Hervé et al., 2013). The only directional data currently available in Europe prior to this age come from Eastern Europe (Aidona and Kondopoulou, 2012; Burlatskaya et al., 1986; Márton, 2009; Kovacheva et al., 2009). One of the reasons that explain this lack of data is the unknown of well-dated materials suitable for these chronologies. It is therefore necessary to explore new materials meeting the necessary requirements in order to extend temporally and geographically the existing secular variations records.

We present here the first archaeomagnetic directions obtained from a new geomagnetic field recorder: anthropogenic cave sediments. These materials are known in the archaeological literature as *fumiers* and refer to stratigraphic sequences composed of ash, straw and dung (Brochier, 1983). They are produced by the pe-

riodic combustion of domestic livestock dung and consist of alternating burnt dung layers with unburnt dung levels (Fig. 2). By burning, the caves were cleaned from parasites arising from livestock penning, a common practice that is widely documented in the Mediterranean region since the Neolithic (e.g. Angelucci et al., 2009; Boschian, 1997; Boschian and Montagnari-Kokelj, 2000; Brochier, 1983; Brochier et al., 1992; Karkanas, 2006; Macphail et al., 1997; Straus and González Morales, 2012; Vergés et al., 2002, 2008). These layers have been traditionally studied from sedimentological and archaeobotanical perspectives. However, with the exception of our previous works (Carrancho et al., 2009, 2012), their suitability as geomagnetic field recorders has not been yet fully explored. The objective of this work is twofold. First, to show the suitability of anthropogenic cave sediments to obtain archaeomagnetic data through a comprehensive palaeomagnetic and rock-magnetic study. Second, to design a European PSV curve for the 6000–1000 yr BC time period exclusively based on archaeomagnetic data. The results obtained and their potential application to dating (Lanos, 2004; Pavón-Carrasco et al., 2011) are discussed.

2. Materials and methods

2.1. Description of anthropogenic cave sediments

Anthropogenic cave sediments are known in the French archaeological literature as *fumiers* or “burnt animal dung layers” (English) and are interpreted as a product of pastoral activities (Brochier, 2002). The main goal of these practices was to disinfect the space and reduce the volume of residues generated by the livestock. The Holocene stratigraphy of these sites exhibits a characteristic succession of burnt levels alternating with other few (or un-)burnt layers, generating sequences of rather variable texture and colour (Fig. 2A–B). This alternation between combustion episodes and unburnt levels generates facies’ groups whose transition may be gradual or abrupt. As a whole they make up thin facies successions of centimetre and even millimetre scale, with sub-horizontal stratification or following the topography of the substrate. Slightly convex morphologies are occasionally observed probably related to the accumulation of waste to be burned. The dimensions, morphology and thickness of the ashes are somewhat variable, reaching up to 2–3 meters long and several centimetres of thickness. In section, they are occasionally observed as lenses with abrupt and/or wedged-shape contours and in most cases as horizontal and regular sheets. The presence of archaeological artefacts (generally poor) within these sequences derived from domestic activities (e.g. pottery) suggests that humans lived with the animals in the caves, although occupying differentiated areas. Most



Fig. 2. Characteristic alternation between burnt and unburnt facies of anthropogenic cave sequences. (A) Neolithic stratigraphic sequence of El Mirador Cave (Sierra de Atapuerca, Burgos). East section of test pit. Total visible thickness of deposit, c. 2 m. (B) Burning episode FU-1 (Unit MIR12) showing the characteristic facies sequence observed in these structures. Thickness of ashes is 8 cm.

probably, burning of residuals was carried out at the same place where animals were penned.

In spite of there being no explicit consensus to describe/classify these deposits it has been addressed through a facies system relatively uniform among sites. This is logical since the formation processes of these anthropogenic sediments are essentially the same and their facies composition is more or less indistinguishable from one site to another (Angelucci et al., 2009). Both in geoarchaeological studies (e.g. Boschian and Montagnari-Kokelj, 2000; Macphail et al., 1997) as well as in our own observations, several characteristic facies in the burnt levels have been identified which we synthesised as follows: white and/or grey ashes of variable thickness (~2–10 cm) over thin (~2 cm) subjacent carbonaceous facies of dark colour with organic material (Fig. 2B).

According to sedimentological studies (Boschian and Montagnari-Kokelj, 2000; Brochier et al., 1992) and experimental dung-burning recreations (Vergès, 2011) this facies arrangement corresponds to a single burning event. The ash thickness essentially depends on the amount of fuel burnt which on the other hand, undergoes a considerable reduction of its initial volume (up to 80%) during combustion (Brochier, 2002; Vergès, 2011). This certainly favoured the compaction and reduced the porosity of ashes. Preservation of these burning events is favoured by the fast sedimentation rates of these deposits, usually of the order of millimetres per year (Angelucci et al., 2009). Each burning event is stratigraphically sealed by the rapid burial of the upper level preventing alteration. The combustion itself is a preservation factor as it inhibits the breakdown of the mineral fraction present in the organic remains (Angelucci et al., 2009). Nevertheless, these deposits may be locally affected by diverse syn- and/or post-depositional processes (e.g. bioturbation), some of them visible at the macroscopic scale. Recent studies propose the palaeomagnetic technique as a useful indicator of post-depositional processes (Carrancho et al., 2012).

2.2. Sites studied

The studied materials correspond to Neolithic, Chalcolithic and Bronze Age burnt levels in “El Mirador” and “El Portalón” Caves (Sierra de Atapuerca, Burgos, Spain) and “El Mirón Cave” (Ramales de la Victoria, Cantabria, Spain) (Figs. 1A, 2, Supplementary Figs. 1–6 and Table 1). Extensive excavations carried out at these sites have exposed stratified deposits rich in archaeological and palaeontological remains of Upper Pleistocene and Holocene age (Carretero et al., 2008; Straus and González Morales, 2012; Vergès et al., 2002, 2008). Specifically, the Holocene series contain numerous burning events (ash lenses) exposed in various stratigraphic sections. We briefly describe here the most relevant stratigraphic, sedimentological and archaeological aspects of interest with regard to the three sites studied. Description will only focus on the Holocene stratigraphy where the burning events sampled are located.

2.2.1. El Mirador Cave

El Mirador Cave (42°20'58" N, 3°30'33" W; 1033 m above sea level) is located on the southernmost slope of the Sierra de Atapuerca (Burgos, Spain; Supplementary Fig. 1). Archaeological works began systematically at the site in 1999 with a test pit (6 m²) in the central sector of the western half, uncovering a stratigraphic sequence with Upper Pleistocene and Holocene levels. The Holocene series contains a significant presence of burnt levels produced by the *in situ* burning of vegetal materials and animal dung, mainly ovicaprines, generated by the use of the cave as fold of domestic livestock (Vergès et al., 2002, 2008). El Mirador is currently one of the most complete, continuous and well-dated anthropogenic cave sequences known in the Mediterranean Europe.

The Holocene stratigraphy is articulated in 24 archaeological units along 5.5 m of depth (Supplementary Fig. 2). Archaeologically, two main sequences can be distinguished: the lower one with 3.5 m of Neolithic units (MIR6–24) and a 1.6 m upper one belonging to the Bronze Age (MIR3–4). The unit MIR5, which separates the Neolithic sequence of the Bronze Age, is a sedimentary hiatus in which the cave was not occupied for about a thousand years (Vergès et al., 2002). Sedimentation rate of Neolithic units is on average of 1 mm/yr, although it reaches peak values of 15 mm/yr between units MIR16–11 (Angelucci et al., 2009). The numerous cases of anatomical connection of skeletal elements documented in the unburnt facies indicate a high preservation degree of the Neolithic levels. Samples collected and analysed correspond to three successive sampling campaigns (2005, 2006 and 2007). Details concerning the sampled burning events, stratigraphic provenance, number of samples as well as the chronological information are compiled in Table 1.

2.2.2. El Portalón Cave

El Portalón de Cueva Mayor (42°20'53" N; 3°31'02" W; 1034 m above sea level) is also part of the archaeo-palaeontological karstic complex of Atapuerca sites (Burgos, Spain). Although isolated studies have been carried out during the twentieth century, systematic excavations have been conducted since year 2000 at the site. A new stratigraphic sequence with Upper Pleistocene and Holocene levels, based on more than thirty radiocarbon dates spanning from 30 000 to 1000 yr BP, has been recently published (Carretero et al., 2008) (Supplementary Fig. 3).

The Holocene infilling contains Mesolithic, Neolithic, Chalcolithic, Early and Middle Bronze Age, Iron Age, Roman and Medieval occupations (Carretero et al., 2008). Its archaeological record consists mainly of pottery, stone and bone tools, personal ornament items, metallic objects and human, faunal and archaeobotanic remains, among others. The site seems to have worked a long time as habitat area, including activities of animal penning at the upper levels as well as sepulchral space at other times. The stratigraphic sequence consists of 11 levels distinguishing two main different units: Pleistocene (level 10) and Holocene (levels 9 to 0). The Holocene unit with a maximum thickness of 630 cm is composed

Table 1

Mean archaeomagnetic directions obtained in the burning events sampled at the three sites (see notes at bottom.)

EL MIRADOR CAVE (S. de Atapuerca, Burgos). 42°20'58" N LAT; 3°30'33" W LONG										
Burning event	Archaeological unit	Section	t_{min}	t_{max}	t_{mean}	N/N'	Dec. (°)	Inc. (°)	α_{95} (°)	k
N2-MSE01	Mir9	East	4330	3650	3990	16/21	9.4	53.7	6.1	38.0
N4	Mir9	East	4330	3650	3990	7/9	15.2	56.0	8.0	57.4
N5-MSE02	Mir10	East	4330	3790	4060	10/16	357.9	56.0	6.8	50.7
N6-MSE04	Mir12	East	4440	4050	4247	21/37	15.3	42.6	4.0	63.3
FU1	Mir12	West	4440	4050	4247	22/28	336.8	52.8	4.7	43.8
N7-MSE06	Mir13/14	East	4450	4240	4345	12/18	6.3	51.7	4.9	79.5
FU2-MSE08	Mir15	South	4710	4250	4480	15/24	3.2	54.4	5.7	46.7
N8	Mir15	East	4710	4250	4480	14/20	12.9	42.2	6.5	38.7
N9-MSE09	Mir16	East	5210	4250	4730	28/40	14.5	54.6	2.6	109.1
N10-MSE10	Mir16 _{inf}	East	5210	4250	4730	11/19	19.0	53.3	3.6	157.9
N11-MSE11	Mir16	East	5220	4370	4795	9/22	17.9	51.3	4.4	136.5
FU4	Mir21	West	5220	4860	5040	14/17	335.4	65.6	3.9	103.1
N15	Mir22	East	5470	4860	5165	12/18	8.1	54.4	3.0	211.3
N16	Mir22	East	5470	4860	5165	9/18	359.9	61.0	3.6	202.0
N18-MSE15	Mir23	East	6020	5000	5510	19/25	10.5	58.7	3.5	95.4
EL MIRÓN CAVE (Ramales de la Victoria, Cantabria). 43°14'48" N LAT; 3°27'05" W LONG										
Burning event	Archaeological unit	Zone	t_{min}	t_{max}	t_{mean}	N/N'	Dec. (°)	Inc. (°)	α_{95} (°)	k
RM5	between 3 and 5	OV	2900	1970	2435	7/11	9.3	64.8	5.3	130.1
RM13	4	MV	2900	1970	2435	10/11	346.7	54.0	6.8	51.9
RM2	9.8	OV	4690	3710	4200	8/13	343.5	54.9	4.3	90.0
RM8	between 303 and 303.2	MV	4540	4070	4305	8/12	350.1	47.4	5.1	119.4
RM11	303.1–303	MV	4540	4070	4305	10/15	357.8	49.6	12.0	17.2
RM9	303.3–303.2	MV	4460	4240	4350	8/10	354.3	50.3	5.8	92.4
RM15	303.3	MV	4500	4340	4420	9/14	345.9	52.4	4.7	123.5
RM10	below 303.3	MV	4870	4340	4605	10/11	353.6	46.5	5.1	90.0
EL PORTALÓN CAVE (S. de Atapuerca, Burgos). 42°20'53" N LAT; 3°31'02" W LONG										
Burning event	Archaeological unit	Zone	t_{min}	t_{max}	t_{mean}	N/N'	Dec. (°)	Inc. (°)	α_{95} (°)	k
P3	between 1 and 1/2	North	780 (BC)	1020 (AD)	120 (AD)	19/24	340.2	57.4	3.1	116.9
P2	4inf/5	NE-B8	2290	1920	2105	19/27	352.0	69.7	4.1	67.0
P1	4inf/5	NE-B8	2400	2040	2220	11/16	12.9	50.9	4.6	101.2

Notes. From left to right: t_{min} , minimum age in cal. yr BC; t_{max} , maximum age in cal. yr BC; t_{mean} , mean age in cal. yr BC; N/N' : number of specimens considered for the calculation of the mean direction (N)/number of specimens oriented and analysed from the site (N'); Dec. (declination), Inc. (inclination); k and α_{95} , precision parameter and confidence limit of ChRM at the 95% level (after Fisher, 1953).

of relatively homogeneous sediments and is rich in archaeological remains. Sampled materials correspond to three burning events exposed in the North and Northeast sections of the Holocene stratigraphy. Their stratigraphic and chronological details are compiled in Table 1. A total of 67 oriented specimens of ash and carbonaceous samples were collected. Occasionally, mechanical alterations of the sediment induced by bioturbation were identified. However, these are well-located and the preservation state of the burning events can be considered as good.

2.2.3. El Mirón Cave

El Mirón Cave (43°14'48" N, 3°27'05" W; 260 m above sea level) is located in the upper valley of the Asón river (Ramales de la Victoria, Cantabria, Spain). Archaeological excavations since 1996 have documented a long cultural sequence with levels spanning the late Middle Palaeolithic to the early Bronze Age, including also traces of medieval and modern activities. Currently, the site has 78 radiocarbon dates ranging from 41 000 BP (uncal.) to AD 1400 (Straus and González Morales, 2003, 2007, 2010, 2012).

The excavations have focused on two areas of around 9 m² in the vestibule of the cave: Outer Vestibule (OV – Cabin Area) and another at the rear (Vestibule rear, VR – Corral), connected by a 9 × 1 m trench (Mid-Vestibule, MV; Supplementary Fig. 4). A 3 m² test pit was also dug in the Vestibule rear, at the foot of an alluvial ramp leading to the inner part of the cavity. Together with Late Mousterian, Gravettian, Solutrean, Magdalenian, Azilian, Mesolithic, Neolithic, Chalcolithic and Bronze Age visits or

occupations have been documented. Stratigraphic, sedimentological and chronological details of El Mirón have extensively reported elsewhere (Courty and Vallverdú, 2001; Cuenca-Bescós et al., 2008; Straus et al., 2001; Straus and González Morales, 2003, 2007, 2010, 2012), to which we refer for details of the Pleistocene succession. The burning events sampled correspond to the Neolithic, Chalcolithic and Bronze Age levels and were identified in the Cabin Area (OV; Supplementary Fig. 5) and in the adjacent Trench (MV; Supplementary Fig. 6). Neolithic occupations were identified in the OV (Cabin, levels 8–10) and in the West section of the adjacent Trench (MV, levels 303–303.3). The Neolithic levels of the Trench mainly consist of a series of well-defined burnt levels with pottery, lithic and domesticated animal remains (mainly sheep/goat). In level 303.3, an individual charred grain of wheat (*Triticum dicocum*) was dated to 5500 BP (~4400 cal. BC), providing the oldest direct evidence of agriculture in the Cantabrian region (Peña Chocarro et al., 2005). The Mid-Vestibule Trench levels 303–303.3 physically correlate with OV levels 10–8, dated between 4600 and 3500 cal. BC (Straus and González Morales, 2003).

The Chalcolithic levels (7–4) in the OV consist of a massive succession of ash and charcoal lenses. The Chalcolithic attribution is based on the available dates and by the typology of artefacts (including characteristic arrowheads), with an age of around 2500 cal. BC (Straus and González Morales, 2003). OV levels 2 and 3 correspond to Bronze Age with an estimated age of around 2100 cal. BC (Straus and González Morales, 2003). They contain pottery fragments, domesticated animal remains (especially cattle), a copper

pin and evidences of *in situ* burning related with metallurgical activities. A total of 191 oriented burnt samples from 15 burning features were collected at the site. Details about their stratigraphic provenance, corresponding archaeological unit and ages considered are compiled in Table 1.

2.3. Sampling

Due to their non-consolidated nature, these materials could not be sampled with standard archaeomagnetic techniques so we developed an alternative sampling technique. The device consists of a non-ferromagnetic metal tube incorporating a built-in orientating system which allows a precise geographical orientation of the samples (Supplementary Fig. 7). The device is carefully inserted in vertical stratigraphic sections where the burning events are exposed. The samples are subsequently saved in cylindrical plastic boxes (3.6 cm³) for alternating field (AF) demagnetisation and stored at low temperatures (3–4 °C) until measurement to avoid chemical alterations. Similarly, representative samples for each fire were introduced by the same means into home-made plaster cubes designed for thermal demagnetisation of the natural remanent magnetisation (NRM). The plaster cubes contain a cylindrical hole with the same dimensions and volume than the plastic capsules in order to keep motionless the sample (Carrancho, 2010). Afterwards, in the lab they were properly sealed and consolidated to carry out thermal demagnetisation. The consolidation was only performed on samples collected for thermal demagnetisation which were impregnated during some days in ethyl-silicate (commercial name Silbond 40) and left to dry during 3–4 weeks. The NRM of the cubes was around two orders of magnitude lesser than the sample's magnetisation. 662 oriented specimens corresponding to 39 burning events (ash–carbonaceous couplets) from the three sites with an average of 16 samples per fire were collected (Table 1).

2.4. Age of the materials

The ages of the investigated structures range from 5500 to 2000 yr cal. BC, but are mostly comprised between 5500 and 4000 BC (Table 1). They have been determined through radiocarbon dates on fragments of charcoal, charred seed, animal bone (one sample from Portalón Cave), tooth or organic sediment (Accelerator Mass Spectrometry – AMS, conventional or extended count). Samples from “El Mirador” and “El Portalón” Caves were analysed at Beta Analytic Inc. Laboratory (Florida, USA) and those from “El Mirón Cave” by Geochron Laboratories (Massachusetts, USA). Ages are expressed in years BC, at a $\pm 2\sigma$ and were calculated using Calib 6.0 based on Reimer et al. (2009) (Table 1). Overall, standard deviations are mostly < 50 yr at a 2σ range which is very acceptable. Only some dates from El Mirón cave – associated to conventional or extended count radiocarbon dating – show larger standard deviations but coherent with ages from the same stratigraphic unit. Therefore, chronological adscription is highly reliable. For the three sites, we considered as chronological criteria the minimum and maximum calibrated radiocarbon ages of the upper and lower stratigraphic level, respectively.

According to this criterion, several burning events sampled within the same archaeological unit share a maximum and minimum age interval (Table 1). This is the case of various structures sampled between units 303.3 and 303 at “El Mirón Cave” and in units MIR9, 12, 15, 16 and 22 at “El Mirador Cave”. Two burning events in “Portalón Cave” (P1 and P2) correspond to the same archaeological unit. However, their stratigraphic location and the many dates available enable us to constrain well their age. Fortunately, both at “El Mirador” and “El Mirón”, the lateral continuity of some facies allow establishing stratigraphic correlations/differentiations among the different burning events. Specifically at “El

Mirón”, the six datings corresponding to the early Neolithic levels (303.3–303/10; Table 1), suggest a fast sedimentation (Straus and González Morales, 2007), probably in not more than 500 yr.

2.5. Palaeomagnetic and rock-magnetic methods

Palaeomagnetic and rock-magnetic analyses were carried out at the Laboratory of Palaeomagnetism of Burgos University (Spain). Magnetic remanence measurements were made with a three-axis 2G SQUID cryogenic magnetometer (noise level $\sim 5 \times 10^{-12}$ Am²). The NRM stability was analysed both by progressive alternating field (AF) and thermal demagnetisation. Stepwise progressive AF demagnetisation was done in 15–17 steps up to 100–120 mT. Thermal demagnetisation was carried out in 16 heating steps up to 680 °C using a TD48-SC (ASC) thermal demagnetiser. Low-field magnetic susceptibility was measured initially and after each heating step with a KLY-4 Kappabridge (AGICO, noise level 3×10^{-8} S.I.) to monitor magneto-chemical alterations. Characteristic Remanent Magnetisation (ChRM) directions were calculated by linear regression of the component that linearly converges towards the origin over five demagnetisation steps. Mean directions and associated statistical parameters were calculated using Fisher's (1953) statistics.

In order to further study the magnetic properties of these materials, representative ash and carbonaceous samples from all sites were selected to carry out a full set of rock-magnetic experiments. With the aid of a Variable Field Translation Balance (MM_VFTB) we measured: progressive isothermal remanent magnetisation (IRM) acquisition curves, hysteresis loops (± 1 T), backfield curves and thermomagnetic curves up to 700 °C in air. Representative ash and carbonaceous samples from “El Mirador Cave” were also selected to carry out thermal demagnetisation of the IRM in three orthogonal axes following Lowrie's (1990) method. The applied fields were 2 T, 0.4 T and 0.12 T for Z, X and Y axes, respectively. Thermal demagnetisation was carried out in 16 temperature steps distributed between room temperature and 680 °C.

3. Results

3.1. Stability of NRM and quality selection criteria

The natural remanent magnetisation (NRM) both of ashes and carbonaceous facies exhibits two distinctive but reproducible behaviours in the three sites. All samples from both facies show a secondary viscous component easily removable in the first steps of the magnetic cleaning (< 10 – 15 mT or < 150 – 200 °C; Figs. 3 and 4), being particularly significant in the carbonaceous. The ashes mostly display a well-defined and stable normal polarity magnetic component which decays univectorially towards the origin, being of high intensity and almost demagnetised at 80–100 mT (Fig. 3A–C). Ashes thermally demagnetised define their characteristic remanent magnetisation (ChRM) between 250 °C and 580–600 °C (Fig. 3D–E). The carbonaceous samples AF demagnetised show in most cases a single normal polarity magnetic component (Fig. 4D and F). Occasionally, however, several components partially overlapping can be distinguished (Fig. 4A and B). By thermal demagnetisation it is revealed the presence of partial thermoremanences (p-TRM) in this facies with maximum unblocking temperatures (T_{ub}) in the range of 350–450 °C (Fig. 4C, E and G). This component was considered as the ChRM direction defined between 200 and 350–450 °C. In these samples, a high-temperature (400–600 °C) component is observed as insets of Fig. 4E and G illustrate. It is interesting to note that mean directions both of ashes and carbonaceous samples calculated separately in each burning event are coincident. This reinforces the idea that both facies

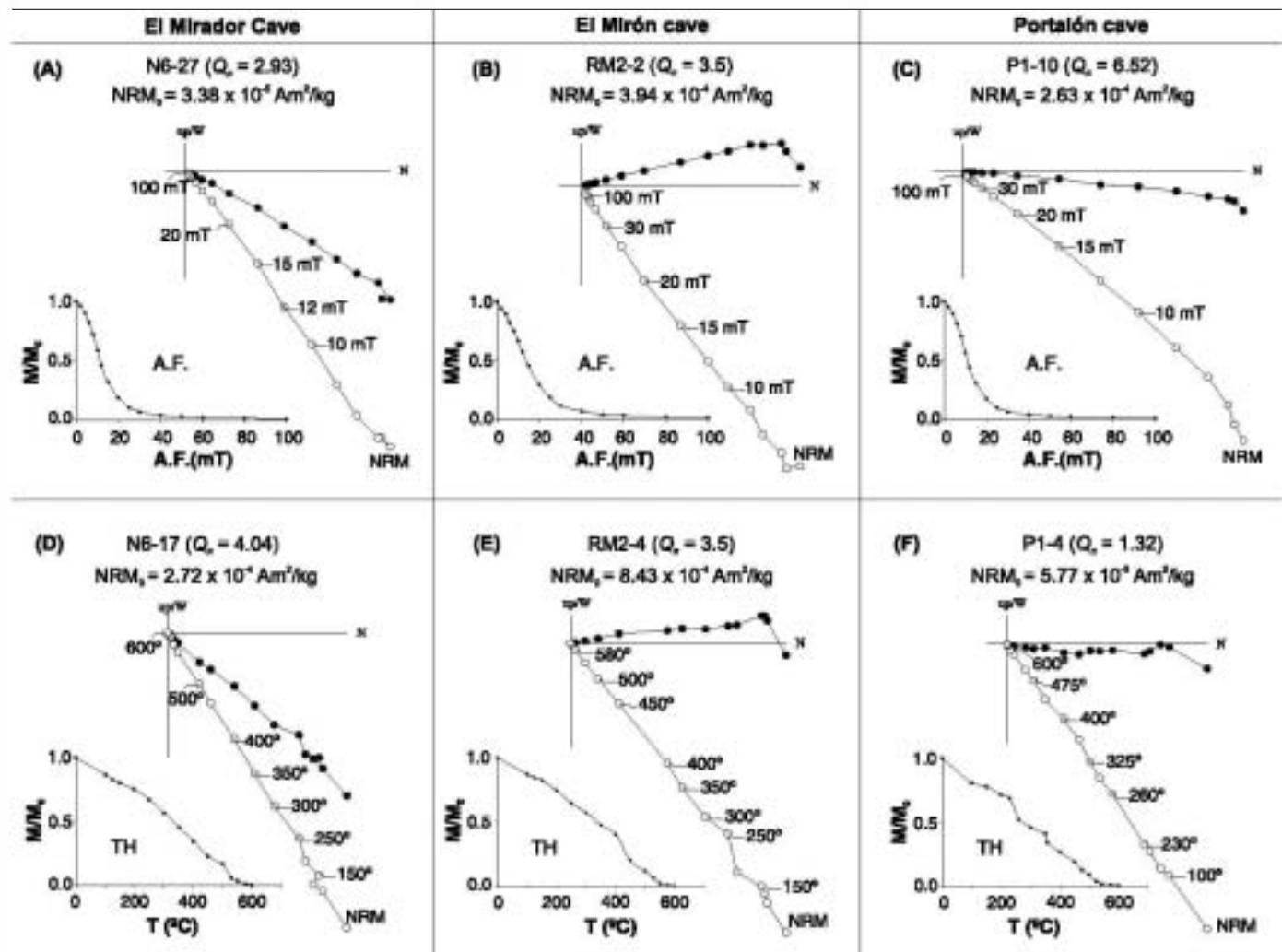


Fig. 3. Representative orthogonal NRM demagnetisation plots for six ashes from the three sites. Open (closed) symbols represent the vertical (horizontal) projections of vector endpoints. The sample code, intensity (NRM_0), Koenigsberger (Q_n) ratio and demagnetisation spectra are indicated for each sample. (A–C) AF = alternating field; (D–F) TH = thermal. Diagrams from both techniques correspond to the same burning event.

recorded faithfully the geomagnetic field direction at the time of burning.

In contrast to the good palaeomagnetic properties of most investigated structures, some showed anomalous behaviour which is related to mechanical alterations. As we initially did not know the magnetic behaviour of these burning events, our field-work strategy comprised the sampling of every burnt structure or that at least might show signs of have been heated regardless of its thickness and degree of preservation. Thus, there is a clear correlation between the quality of the archaeomagnetic data obtained and a good preservation of the structure. In those burning features showing anomalous behaviour (e.g. multicomponent NRM demagnetisation diagrams in ashes with anomalous or highly scattered directions), we have found to converge a number of evidences common to the three sites indicative of sediment reworking. These are ashes mixed with unburnt sediment, occasional absence or discontinuities in the carbonaceous facies, a small thickness in the ashes and Koenigsberger (Q_n) values (Stacey, 1967) < 1. All these features are indicative of disturbance by mechanical removal of the ashes (e.g. bioturbation) as Carrancho et al. (2012) observed in a previous study at El Mirador Cave. The subsequent movement of the ferromagnetic (s.l.) particles reduces the remanence maintaining the susceptibility therefore generating low values of the Q_n ratio and multicomponent NRM diagrams. Likewise, the partial or

total absence of the subjacent carbonaceous substrate as well as irregular geometries in the facies comprising these burning events are also indicative of mechanical alteration.

We therefore established a set of criteria as a “quality control” in order to identify anomalous behaviours and determine the reliability of these structures to obtain archeomagnetic directions. These are: (i) Presence of all the sedimentary facies for each burning event (ashes over underlying carbonaceous facies); (ii) Koenigsberger (Q_n) ratio values > than unity indicating a stable thermoremanence (TRM) or a partial TRM; (iii) absence of any indication of mechanical alteration in the sediments (e.g. mixed or truncated facies), and (iv) a majority of demagnetisation diagrams with univectorial NRM among the ashes. After applying the selection criteria 13 burning events (6 from El Mirador and 7 from El Mirón not shown in Table 1) were rejected. 347 samples passed the quality control, from which 26 new archaeomagnetic directions corresponding to 26 burning events were obtained (Table 1 and Fig. 5).

3.2. Magnetic properties

The magnetic properties results reported here are referred to representative ash and carbonaceous samples from all sites. Magnetic properties of four Neolithic burning events from “El Mirador

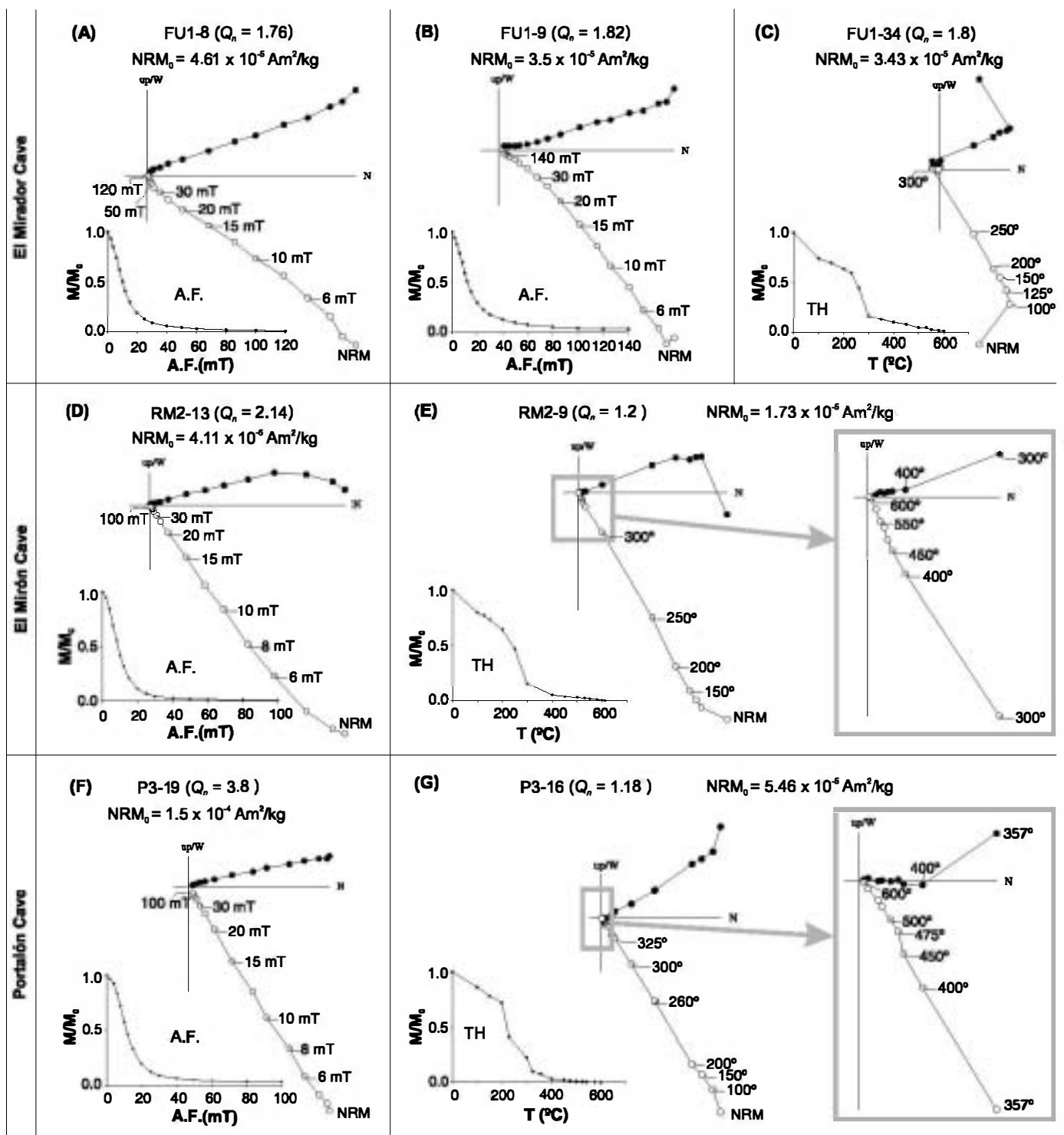


Fig. 4. Representative orthogonal NRM demagnetisation plots for seven carbonaceous samples from the three sites. Symbols are as in Fig. 3. The final steps of the diagrams shown in panels (E) and (G) are blown up to denote the presence of a high-temperature component between 400 and 600 °C.

Cave” – including their supra – and subjacent unburnt levels – were published elsewhere (Carrancho et al., 2009).

3.2.1. IRM acquisition curves and hysteresis cycles

Isothermal remanent magnetisation (IRM) progressive acquisition curves (1 T) are almost saturated around ~150–200 mT, which indicates remanence is carried by low-coercivity ferromagnetic minerals (Fig. 6A, C and E). Hysteresis loops of ashes and carbonaceous samples (expressed on a mass-specific basis and cor-

rected by the paramagnetic fraction), are practically closed around ± 150 mT (Fig. 6B, D and F) again indicating the dominant presence of low-coercivity minerals. All samples exhibit pseudo-single domain (PSD) hysteresis parameters according to Day et al. (1977). The main difference between both facies is the intensity of magnetisation: notably higher in ashes than carbonaceous samples. Occasionally, however, similar intensity values between both facies can also be observed (e.g. Fig. 6E and F). This characteristic behaviour is reproducible in all studied samples from the three sites.

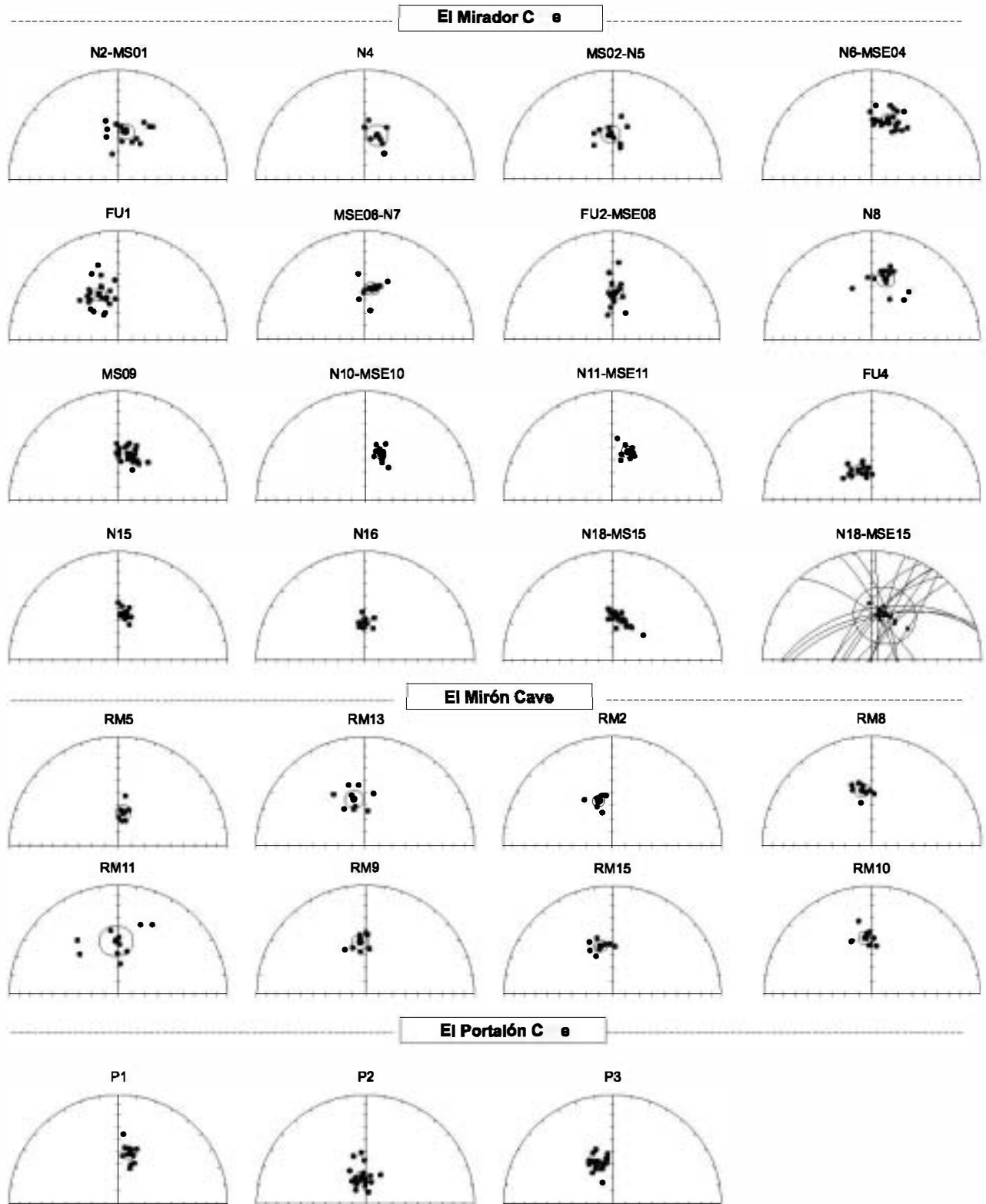


Fig. 5. Equal-area projections of all ChRM directions together with the mean direction and α_{95} for each of the studied burning events accepted. Mean direction of burning episode N18-MSE15 (El Mirador) has also been calculated with remagnetisation circles.

3.2.2. Three-axial thermal demagnetisation of IRM

The soft magnetic component (<0.12 T) shows maximum unblocking temperatures (T_{ub}) of ~ 575 – 625 °C, indicating the presence of magnetite and/or magnetite partially maghaemited (Supplementary Fig. 8). We cannot exclude the presence of stable

maghaemite with respect to the inversion to haematite (Özdemir and Banerjee, 1984), because there is still remanence over 600 °C. The low-coercivity component is dominant in all samples, compared with the magnetisation of the intermediate (0.12–0.4 T) and hard (0.4–2 T) components.

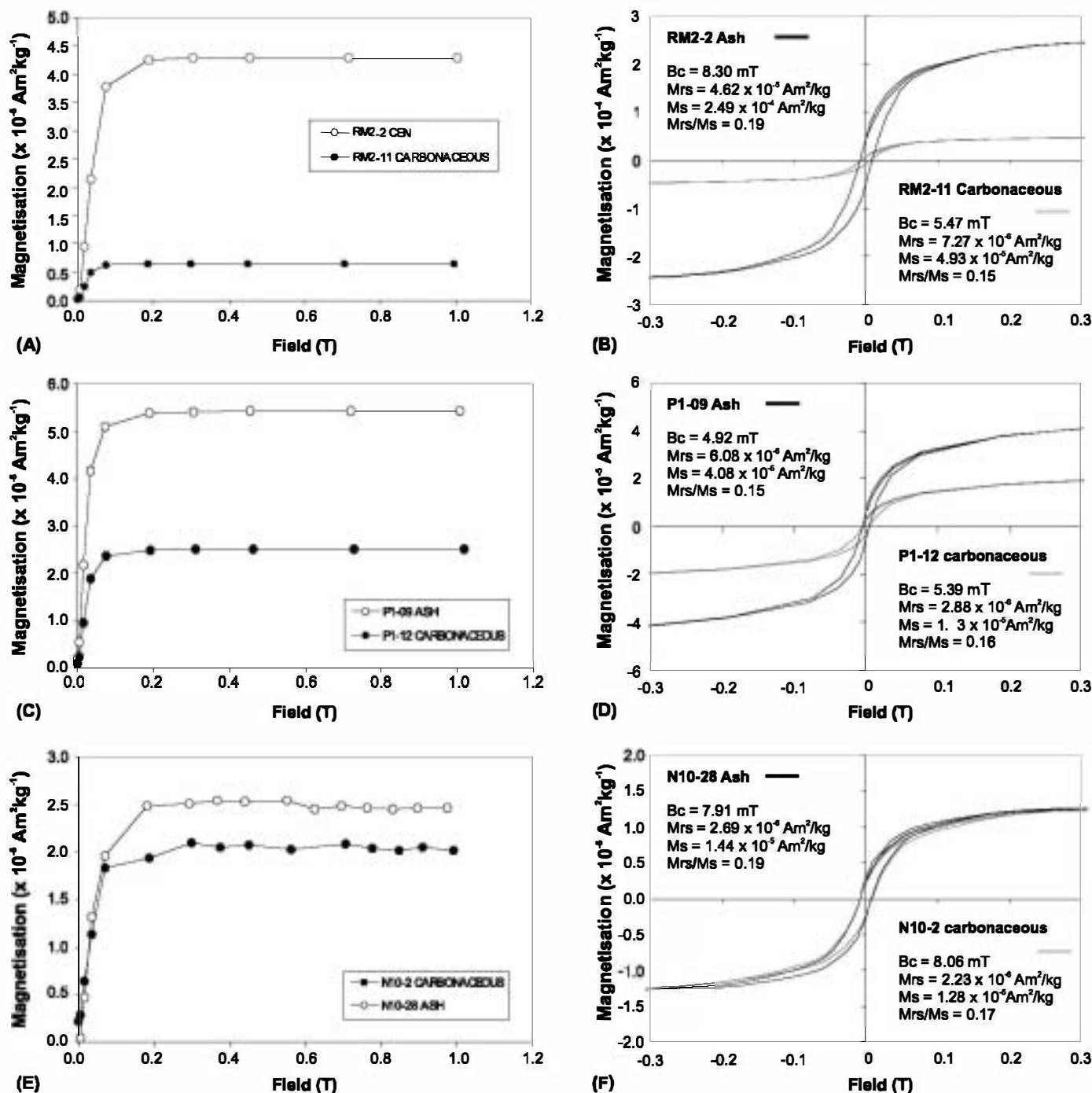


Fig. 6. (A, C and E) IRM acquisition curves and (B, D and F) hysteresis loops of representative ash and carbonaceous samples from the three sites. Intensity values and some hysteresis parameters are indicated. Maximum applied field of hysteresis loops was $\pm 1 \text{ T}$ but for clarity we show the results up to $\pm 0.3 \text{ T}$ (main part of the cycles).

3.2.3. Thermomagnetic curves

Magnetisation variations at temperatures up to 700°C (J - T curves) in representative ash and carbonaceous samples, show that the main magnetic carrier is magnetite or slightly substituted magnetite, with Curie temperatures (T_c) around 580°C (Fig. 7A-B and E-I). Occasionally, some ashes show slightly higher Curie temperatures (e.g. Fig. 7C and D), which are interpreted as magnetite partially maghaemited. The inflexion at intermediate Curie temperatures of ~ 250 – 300°C observed in the heating and cooling cycles of some ashes (e.g. Fig. 7E and F) are probably related with stable maghaemite or less likely, a strongly isomor-

phous substituted spinel phase. We have not observed apparent relation between the colour of ashes and their thermomagnetic behaviour. The ashes display a high degree of reversibility, which indicates that they underwent high-temperature heating. Carbonaceous samples, however, increase considerably the magnetisation on cooling from 580°C , indicating the creation of secondary magnetite (e.g. Fig. 7G-I). The intensity of magnetisation among samples is variable but the highest values are found in ashes because concentration of ferromagnetic minerals is higher than in the carbonaceous ones. Both ashes and carbonaceous samples show a distinctive but reproducible behaviour.

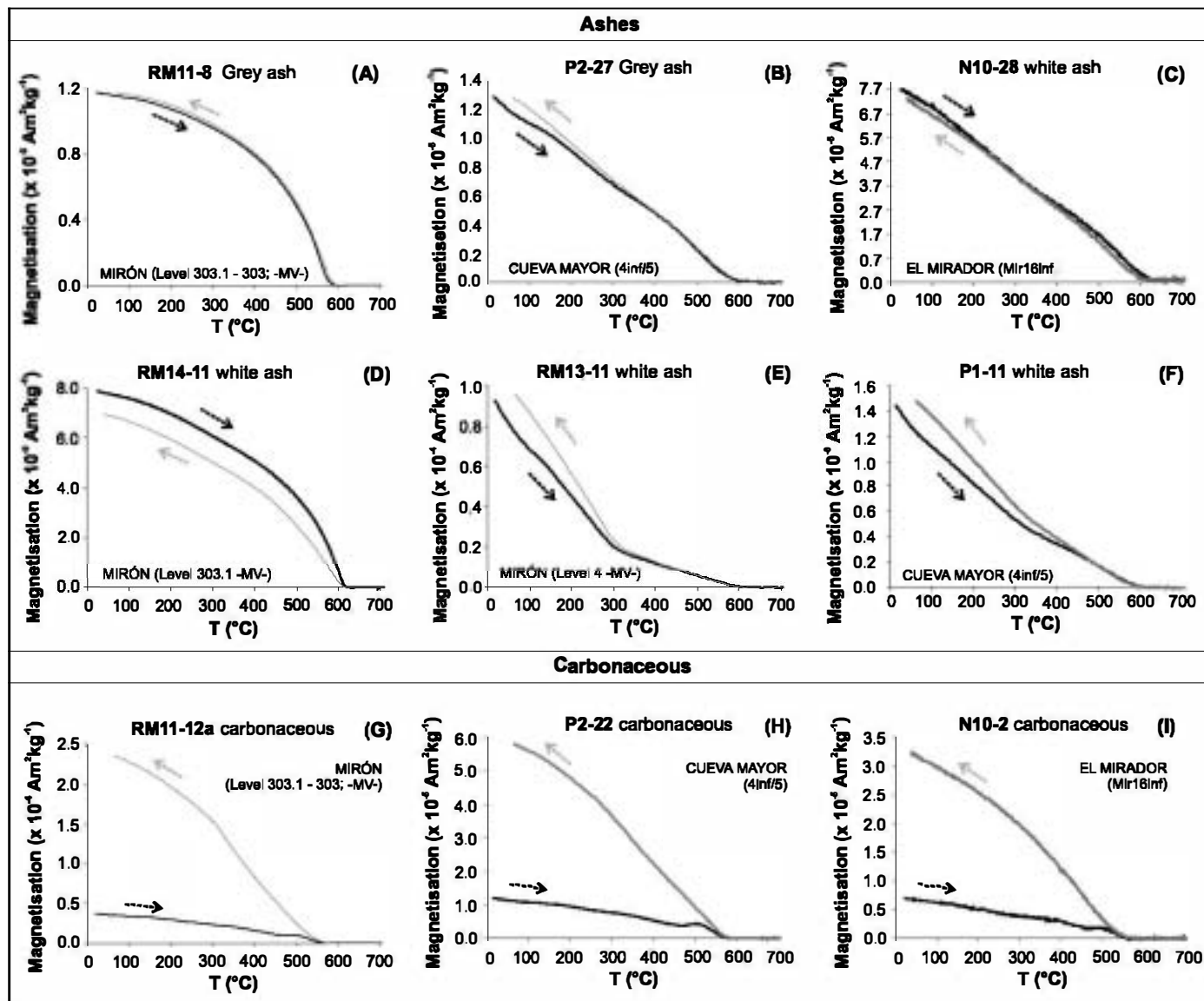


Fig. 7. Representative examples of thermomagnetic curves (J vs. T) of (A–F) ashes and (G–I) carbonaceous samples from the three sites. Heating (cooling) cycles are plotted in black (grey) with their respective arrows. Sample code, site, archaeological unit, ash colour and intensity of magnetisation are indicated. Note that carbonaceous samples shown in panels (G)–(I) correspond to the same burning event as the ashes shown in figures (A)–(C).

4. Discussion

4.1. Origin of the NRM in fumiers

In summary, the burnt facies studied at the three sites are all dominated by pseudo-single domain (PSD) low-coercivity ferromagnetic minerals (magnetite, slightly substituted magnetite and/or maghaemite). Although magnetite – with a small amount of isomorphous substitution – is dominant, some results suggest the occasional presence of maghaemite. It has been particularly detected in some thermomagnetic curves (e.g. Fig. 7D) as well as in the thermal demagnetisation diagrams of the NRM with maximum T_{ub} slightly over 600°C (e.g. Fig. 3D). Our interpretation about the mechanism of magnetisation implies that those burning events where magnetite was created by burning at high temperatures, recorded the geomagnetic field through the acquisition of a thermoremanence (TRM). This magnetite was created by burning under reducing conditions with presence of organic matter. The reversibility of the thermomagnetic curves also supports a TRM origin of the magnetisation, but a thermochemical rema-

nent magnetisation (TCRM) cannot be excluded given that stable maghaemite has also occasionally been observed. In such a case palaeointensity determinations would not be valid, although directional data would be valid because the burning and oxidation are closely confined in time (Carrancho et al., 2009). The high degree of reversibility of thermomagnetic curves suggests that ashes underwent high heating temperatures ($> 700^{\circ}\text{C}$). In contrast, the maximum unblocking temperatures (T_{ub}) of the p-TRMs identified in the carbonaceous samples reveal that this facies underwent lower heating temperatures ranging between 350 and 450°C (Fig. 4G, E). The irreversibility of their thermomagnetic curves is also an indication of it (Fig. 7G–I). These observations are not only interesting from the archaeomagnetic point of view but also from the archaeological perspective. Overall, these results agree well with those obtained at the Neolithic levels of El Mirador Cave (Carrancho et al., 2009). A considerable number of specimens had to be rejected because they were affected by mechanical disturbance processes. Therefore it is important to apply the selection criteria proposed here when studying anthropogenic cave sediments for archaeomagnetic analysis.

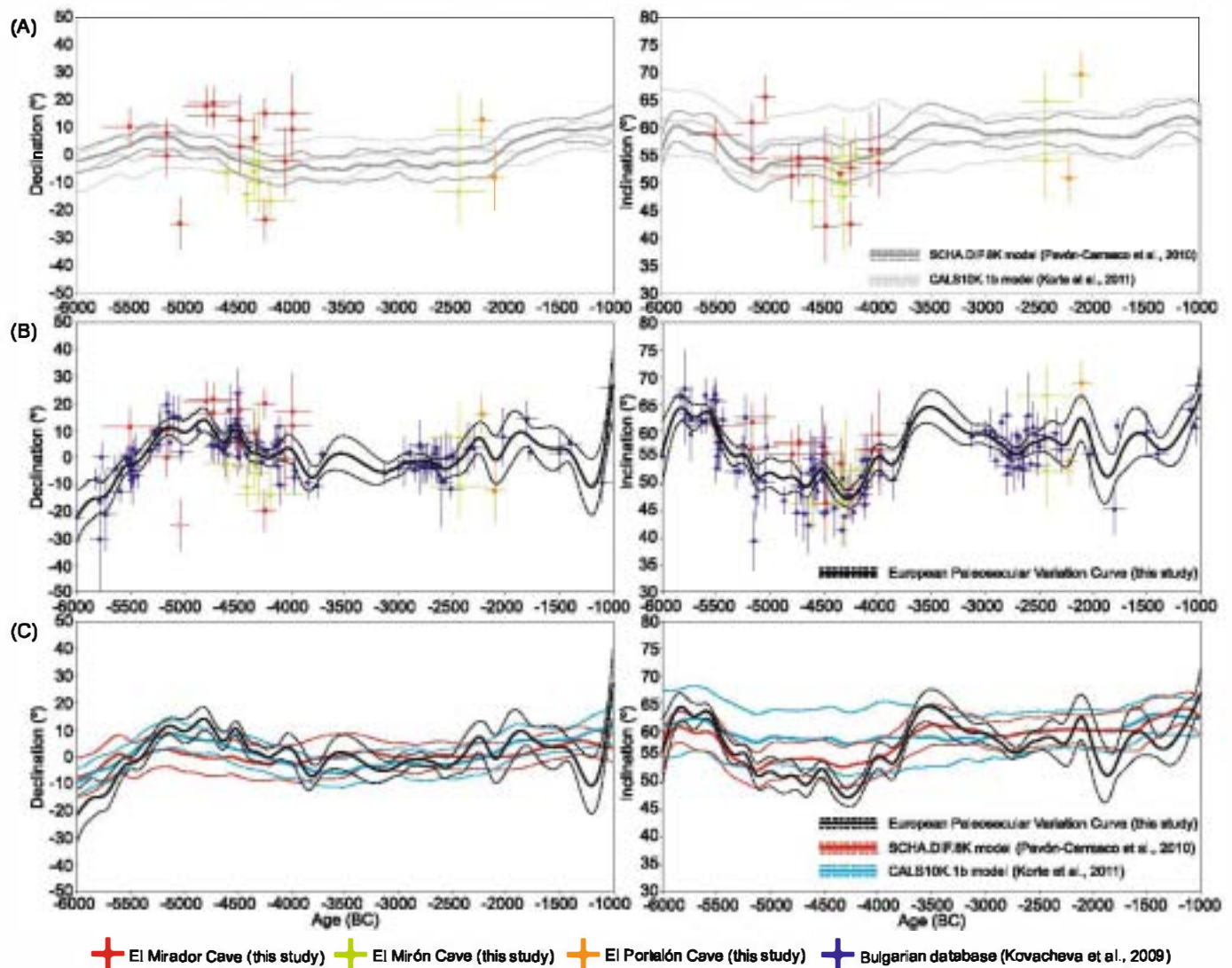


Fig. 8. Comparison between the data, the master curve and model predictions. (A) The new data and the model predictions at 42.35° N, 3.51° W. (B) The new master curve and the input data. (C) The master curve and the model predictions. In (B) and (C) all data and models at 43.0° N, 11.0° E.

4.2. First Neolithic directional results from Western Europe

The archaeomagnetic data reported here represent the oldest directional results from burnt archaeological materials throughout all Western Europe. From the 39 sampled structures at the three sites it has been reported 26 well-defined archaeomagnetic directions: 15 directions were obtained from El Mirador, 8 from El Mirón and 3 from El Portalón (Fig. 5). Mean directions, statistical parameters and their associated age intervals are compiled in Table 1. Mean directions have been calculated with a minimum of 7 samples, the dispersion parameter (k) is reasonably acceptable and in 24 out of 26 data the α_{95} is comprised between 3 and 6.9° (Table 1). Data from 13 structures (6 from El Mirador and 7 from El Mirón Cave) were rejected because they did not pass the quality criteria described in Section 3.1. Burning events FU1 (Mir12) and FU4 (Mir21) from the West section of El Mirador Cave (Table 1), have the most aberrant directions showing significant directional deviation in comparison with coetaneous burning events from the East Section. However, no apparent tectonic deformation was observed in the field and they fulfil the quality selection criteria established in Section 3.1, so they were not excluded. Although some scatter is observed in the data (Fig. 8A), higher than in com-

mon archaeological heated structures (as ceramic kilns), coherence in directional results among sites is also evidenced.

4.3. Comparison with global and regional models

The new archaeomagnetic data reported here have been compared with the two secular variation models available for these ages: the CALS10K.1b global model (Korte et al., 2011) and the European regional model SCHA.DIF.8K (Pavón-Carrasco et al., 2010). The first one covers the last 10 millennia (8000 BC–1990 AD) compiling directional and intensity data from archaeomagnetic materials, lava flows and lacustrine sediments studied worldwide. The second model (SCHA.DIF.8K) includes archaeomagnetic and sedimentary data for the last 8 millennia exclusively from Europe. Due to the scarcity of archaeomagnetic data both models include materials of different origin whose magnetisations are acquired through different mechanisms. That is, both models include sedimentary records that produce the already mentioned “smoothing effect” which should be taken into account when comparing with burnt archaeological material, carrying a TRM acquired in a brief time interval.

The directions reported here – mostly concentrated between ~5500 and 4000 yr cal. BC – follow the general trend predicted

by the models but displaying higher variability (Fig. 8A). In particular the data comprised between ~ 4200 and 4600 BC, show a clear tendency towards lower inclinations than the synthetic curves. The smoothing effect of the models does not allow a precise comparison with the archaeomagnetic data obtained in the anthropogenic cave sequences. This effect is particularly noticeable in Western Europe where only lacustrine records were available for these ages. Low inclinations are also observed for the same time interval in the archaeomagnetic Bulgarian database (Kovacheva et al., 2009) (Fig. 8B). The lower variability in inclination predicted by the models is then attributed to the smoothing effect produced by using sedimentary records in the models construction as input data. We do not consider that the low inclination values are due to compaction effects, since the observed variations in inclination are inhomogeneous through time. Moreover, the oldest and stratigraphically deepest data in the studied sequences that theoretically endured higher lithostatic charges should have produced lower inclinations and this is not the case. In fact, the oldest data show inclination values substantially higher than those comprised between 4200 and 4600 yr cal. BC (Fig. 8A).

4.4. First European PSV curve for the Neolithic

In order to develop a European PSVC based exclusively on archaeomagnetic data, the new data presented here and the Bulgarian archaeomagnetic database were relocated to a common intermediated location, i.e. 43° N/ 11° E, by using the virtual geomagnetic pole method (Noël and Batt, 1990). The consistency of this new European archaeomagnetic database allows us to propose the first European archaeomagnetic PSVC (Fig. 8B). In order to obtain the best fitting between the data and the PSVC a bootstrap method was applied (Korte and Constable, 2008; Thébault and Gallet, 2010) using the original values of the database and penalised cubic B-splines in time. The synthetic data for each bootstrap curve were randomly modified by two mathematical distributions: (a) for the directional values, we used a Gaussian random distribution centred in the mean value of the directional data with a standard deviation equal to the directional uncertainties (σ_{65}), and (b) in time, a homogeneous random distribution was used, with minimum and maximum values given by temporal uncertainties at 1σ . The temporal bases of cubic B-splines were calculated with fixed knot points every 50 years from 6000 BC to 1000 BC and regularised by an additional penalty function which controls the trade-off between the input data and roughness of the estimated directional curve. In this case, we have used the second derivative of the function as the penalty function as follows:

$$\hat{f} = (\hat{B}' \cdot \hat{C}^{-1} \cdot \hat{B} + \lambda \cdot \hat{\Phi})^{-1} \cdot \hat{B}' \cdot \hat{C}^{-1} \cdot \vec{y}$$

where \hat{f} is the estimated function, i.e. the calculated palaeosecular variation curve. \hat{B} is the matrix containing the basis of cubic B-splines (\hat{B}' is the transpose of \hat{B}). \hat{C} is the data error covariance matrix and \vec{y} is the vector of input data (declination or inclination data). The matrix $\hat{\Phi}$ is the penalty function which depends on the second time derivative of the estimated function \hat{f} with damping parameter λ . A total of 2000 individual declination and inclination curves were obtained following this procedure. The final directional PSVC was generated using the mean value provided from the average of the 2000 curves and their standard deviations (Fig. 8B and Supplementary Table 1).

The master curve is well constrained between 6000 and 3800 BC (Fig. 8B). Inclination values of about 65° are observed for the oldest data, followed by a progressive decrease, reaching a minimum ($\sim 45^\circ$) around 4200 BC. Declination values vary from -20°

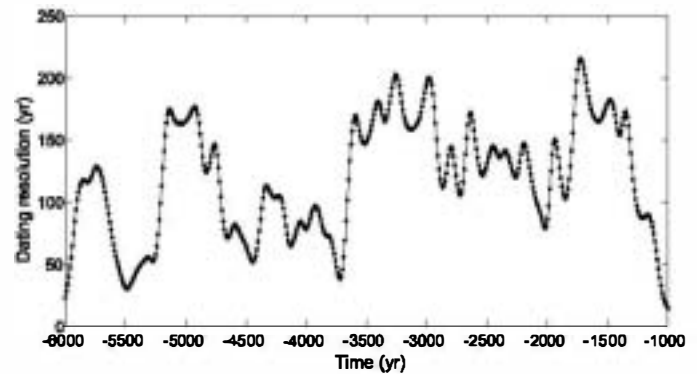


Fig. 9. Dating resolution in years corresponding to the first European directional master secular variation curve for the period 6000 to 1000 yr BC.

to 20° between 6000 and 5000 BC, migrating westward up to values of -10° around 4000 BC. There is a gap of data between 3400 and 3800 BC. The curve is again well-defined between 3300 and 2300 BC, followed by a period of lower data density that is poorly represented.

Fig. 8C illustrates the comparison of the new master curve and the curves predicted by the models (Korte et al., 2011; Pavón-Carrasco et al., 2010). The new curve is contained within the error margin of the synthetic curves provided by the models but it is better defined (lower errors) and indicates a higher frequency in the directional variation of the geomagnetic field for the 6000 – 2000 BC time period than previously suspected. These variations are similar to those observed for the last 3000 yr, the period with the highest density of archaeomagnetic data.

The new master curves can be used as a tool for archaeomagnetic dating from 6000 to 1000 BC. To that aim, it has been included into the PSVC database of the *archaeo_dating* tool software (Pavón-Carrasco et al., 2011) and it is available at <http://earthref.org/ERDA/1134/>. The resolution of an archaeomagnetic date using the master curve depends on time due to the scattering of the data and the directional behaviour of the geomagnetic field itself. To quantify this variation on the resolution, we have dated synthetic mean values of the master curve from 6000 to 1000 BC, using the own master curve and the *archaeo_dating* software. The dating resolution of the curve (6000 – 1000 yr BC) is typically below ± 200 yr and for certain parts of the curve it may reach ± 30 yr (e.g. around 5500 BC) showing a clear correlation with the error of the master curve (Fig. 9). As expected, the maximum resolution is reached in those time intervals with the lowest errors and, in contrast, those intervals less well-defined have less dating resolution. The main implication from the archaeological point of view is that this dating approach may reach similar precision as radiocarbon, although it is clear that still needs to cover some gaps (e.g. 3800 – 3200 BC).

This contribution will benefit diverse disciplines in Earth's Sciences from geophysics (e.g. providing new data to model the geometry of geomagnetic field) to Archaeology (extending back in time the archaeomagnetism as a dating method) or even also palaeoclimatology, since geomagnetic field models are necessary to correct production of cosmogenic isotopes. As long as more archaeomagnetic data will be compiled the resolution and chronological extension of this new curve will be certainly improved.

5. Conclusions

The archeomagnetic and rock-magnetic study of anthropogenic cave sediments from three caves in Spain leads us to the following conclusions:

(1) 26 new archaeomagnetic directions ranging between ~ 5500 and 2000 yr BC have been obtained. These data represent the

oldest archaeomagnetic directions obtained from burnt archaeological materials throughout all Western Europe.

(2) The remanence of the burnt facies studied is carried by PSD low-coercivity ferromagnetic minerals (magnetite, magnetite with no significant isomorphous substitution and/or maghaemite). Rock-magnetic experiments indicate a TRM origin of the magnetisation although a TCRM cannot be excluded in those burning features where maghaemite has been occasionally identified.

(3) Several quality selection criteria have been established in order to identify anomalous archaeomagnetic behaviours (related with mechanical syn/post-depositional processes) and determine the reliability of these structures to obtain archaeomagnetic directions.

(4) A first European archaeomagnetic PSV curve for the Neolithic is proposed using these new data and the recent updated archaeomagnetic Bulgarian database. This new curve defines the directional variations of the geomagnetic field with better resolution than sedimentary records. Its dating resolution oscillates from approximately ± 30 yr to ± 200 yr for the period 6000 to 1000 yr BC, having for the moment similar resolution as radiocarbon dating.

Finally, the wide distribution of anthropogenic cave sediments throughout the Mediterranean area will help to cover geographical gaps in the archaeomagnetic database. Furthermore, being part of continuous, *in situ*, generally well-dated stratigraphic sequences is possible to obtain a largely continuous set of data from the same site. More importantly, they are particularly interesting because they span older ages than other materials traditionally used in archaeomagnetism. Although still few to define a secular variation pattern in detail, this study opens new promising perspectives to extend temporally regional secular variation records and to extend back in time the archaeomagnetic dating tool.

Acknowledgements

This work was supported by the Dirección General de Investigación Científica y Técnica, Spanish Ministry of Science (projects CGL2009-10840, CGL2012-32149, CGL2012-38481, CGL2011-24790 and CGL2009-12703-C03). Á.C. research was funded by the *International Excellence Campus Programme, Reinforcement subprogramme*, of the Spanish Ministry of Education. Special gratitude is devoted to the archaeologists implicated in the excavations at the studied sites and to Mary Kovacheva for her continuous work updating the Bulgarian archaeomagnetic database.

Appendix A. Supplementary material

Supplementary material related to this article can be found online at <http://dx.doi.org/10.1016/j.epsl.2013.08.031>.

References

- Aidona, E., Kondopoulou, D., 2012. First archaeomagnetic results and dating of Neolithic structures in northern Greece. *Stud. Geophys. Geod.* 56 (3), 827–844.
- Aitken, M.J., Hawley, H.N., 1967. Archaeomagnetic measurements in Britain IV. *Archaeometry* 10, 129–135.
- Alexandrescu, M., Courtillot, V., Le Mouél, J.L., 1997. High-resolution secular variation of the geomagnetic field in Western Europe over the last 4 centuries: Comparison and integration of historical data from Paris and London. *J. Geophys. Res.* 102, 20245–20258.
- Angelucci, D.E., Boschian, G., Fontanals, M., Pedrotti, A., Vergès, J.M., 2009. Shepherds and karst: The use of caves and rock-shelters in the Mediterranean region during the Neolithic. *World Archaeol.* 41 (2), 191–214.
- Boschian, G., 1997. Sedimentology and soil micromorphology of the Late Pleistocene and Early Holocene deposits of Grotta dell'Edera (Trieste Karst, NE Italy). *Geoarchaeology* 12, 227–249.
- Boschian, G., Montagnari-Kokelj, E., 2000. Prehistoric shepherds and caves in Trieste Karst (northeastern Italy). *Geoarchaeology* 15, 332–371.
- Brochier, J.E., 1983. Combustion et parage des herbivores domestiques. Le point de vue du sédimentologue. *Bull. Soc. Préhist. Fr.* 80 (5), 143–145.
- Brochier, J.E., 2002. Les sédiments anthropiques. Méthodes d'étude et perspectives. In: *Miskovsky, J.-C. (Ed.), Géologie de la Préhistoire: méthodes, techniques, applications*. Geopré, Paris, pp. 453–774.
- Brochier, J.E., Villa, P., Giacomarra, M., 1992. Shepherds and Sediments: Geoethnoarchaeology of Pastoral Sites. *J. Anthropol. Archaeol.* 11, 47–102.
- Burlatskaya, S.P., Nachasova, L.E., Didenko, E.J., Shelestun, N.K., 1986. Archaeomagnetic Determinations of Geomagnetic Field Elements of the USSR Academy of Sciences. Soviet Geophysical Committee of the USSR Academy of Sciences, Moscow, 168 pp.
- Carrancho, Á., 2010. Arqueomagnetismo y magnetismo de las rocas en registros de fuegos arqueológicos holocenos. PhD thesis. Universidad de Burgos, Spain, 282 pp.
- Carrancho, Á., Villalain, J.J., Angelucci, D.E., Dekkers, M.J., Vallverdú, J., Vergès, J.M., 2009. Rock-magnetic analyses as a tool to investigate archaeological fired sediments: a case study of Mirador cave (Sierra de Atapuerca, Spain). *Geophys. J. Int.* 179, 79–96.
- Carrancho, Á., Villalain, J.J., Vergès, J.M., Vallverdú, J., 2012. Assessing post-depositional processes in archaeological cave fires through the analysis of archaeomagnetic vectors. *Quat. Int.* 275, 14–22.
- Carretero, J.M., et al., 2008. A Late Pleistocene–Early Holocene archaeological sequence of Portalón de Cueva Mayor (Sierra de Atapuerca, Burgos, Spain). *Munibe* 59, 67–80.
- Courty, M.-A., Vallverdú, J., 2001. The microstratigraphic record of abrupt climatic changes in cave sediments of the Western Mediterranean. *Geoarchaeology* 16, 467–500.
- Cuenca-Bescós, G., Straus, L.G., González Morales, M.R., García Pimienta, J.C., 2008. Paleoclima y paisaje del final del cuaternario en Cantabria: Los Pequeños mamíferos de la cueva del Mirón (Ramales de la Victoria). *Rev. Esp. Paleontol.* 23 (1), 91–126.
- Day, R., Fuller, M., Schmidt, V.A., 1977. Hysteresis properties of titanomagnetites: Grain size and composition dependence. *Phys. Earth Planet. Inter.* 13, 260–267.
- Donadini, F., Korte, M., Constable, C.G., 2009. Geomagnetic field for 0–3 ka: 1. New data sets for global modeling. *Geochim. Geophys. Geosyst.* 10, Q06007, <http://dx.doi.org/10.1029/2008GC002295>.
- Fisher, R.A., 1953. Dispersion on a sphere. *Proc. R. Soc. Lond. A* 217, 295–305.
- Gallet, Y., Genevey, A., Le Goff, M., 2002. Three millennia of directional variation of the Earth's magnetic field in western Europe as revealed by archaeological artefacts. *Phys. Earth Planet. Inter.* 131, 81–89.
- Gómez-Paccard, M., et al., 2006. First archaeomagnetic secular variation curve for the Iberian Peninsula: Comparison with other data from Western Europe and with global geomagnetic field models. *Geochim. Geophys. Geosyst.* 7, Q12001, <http://dx.doi.org/10.1029/2006GC001476>.
- Hervé, G., Chauvin, A., Lanos, P., 2013. Geomagnetic field variations in Western Europe from 1500 BC to 2000 AD. Part I: Directional secular variation curve. *Phys. Earth Planet. Inter.* 218, 1–13.
- Jonkers, A.R.T., Jackson, A., Murria, A., 2003. Four centuries of geomagnetic data from historical records. *Rev. Geophys.* 41 (2), 1006, <http://dx.doi.org/10.1029/2002RG000115>.
- Karkanas, P., 2006. Late Neolithic household activities in marginal areas: the micromorphological evidence from the Kouveleiki caves, Peloponnese, Greece. *J. Archaeol. Sci.* 33 (11), 1628–1641.
- Korte, M., Constable, C., 2008. Spatial and temporal resolution of millennial scale geomagnetic field models. *Adv. Space Res.* 41, 57–69.
- Korte, M., Constable, C., Donadini, F., Holmes, R., 2011. Reconstructing the Holocene geomagnetic field. *Earth Planet. Sci. Lett.* 312, 497–505.
- Kovacheva, M., Boyadziev, Y., Kostadinova, M., Jordanova, N., Donadini, F., 2009. Updated archaeomagnetic data set of the past 8 millennia from the Sofia laboratory, Bulgaria. *Geochim. Geophys. Geosyst.* 10, Q05002, <http://dx.doi.org/10.1029/2008GC002347>.
- Lanos, Ph., 2004. Bayesian inference of calibration curves: application to archaeomagnetism. In: *Buck, C., Millard, A. (Eds.), Tools for Constructing Chronologies: Crossing Disciplinary Boundaries*, vol. 177. Springer-Verlag, London, pp. 43–82.
- Lowrie, W., 1990. Identification of ferromagnetic minerals in a rock by coercivity and unblocking temperature properties. *Geophys. Res. Lett.* 17, 159–162.
- Macphail, R., et al., 1997. The soil micromorphological evidence of domestic occupation and stabling activities. In: *Maggi, R., Starnini, E., Voytek, B. (Eds.), Arene Candide: A Functional and Environmental Assessment of the Holocene Sequence Excavated by L. Bernabò Brea (1940–1950)*. Mem. Ist. Ital. Paleontol. Um. 5, 53–88.
- Márton, P., 2009. Prehistorical archaeomagnetic directions from Hungary in comparison with those from south-eastern Europe. *Earth Planets Space* 61, 1351–1356.
- Marton, P., Ferencz, E., 2006. Hierarchical versus stratification statistical analysis of archaeomagnetic directions: the secular variation curve for Hungary. *Geophys. J. Int.* 164, 484–489.
- Noël, M., Batt, C.M., 1990. A method for correcting geographically separated remanence directions for the purpose of archaeomagnetic dating. *Geophys. J. Int.* 102, 753–756.

- Özdemir, Ö., Banerjee, S.K., 1984. High-temperature stability of maghemite. *Geophys. Res. Lett.* 11, 161–164.
- Pavón-Carrasco, F.J., Osete, M., Torta, J., 2010. Regional modelling of the geomagnetic field in Europe from 6000 to 1000 B.C. *Geochem. Geophys. Geosyst.* 11, Q11008, <http://dx.doi.org/10.1029/2010GC003197>.
- Pavón-Carrasco, F.J., Rodríguez-González, J., Osete, M., Torta, J., 2011. A Matlab tool for archaeomagnetic dating. *J. Archaeol. Sci.* 38, 408–419.
- Peña-Chocarro, L., Zapata, L., Iriarte, M.J., González Morales, M.R., Straus, L.G., 2005. The oldest agriculture in northern Atlantic Spain: new evidence from El Mirón Cave (Ramales de la Victoria, Cantabria). *J. Archaeol. Sci.* 32 (4), 579–587.
- Reimer, P.J., Baillie, M.G.L., Bard, E., Bayliss, A., Beck, J.W., Blackwell, P.G., Bronk Ramsey, C., Buck, C.E., Burr, G.S., Edwards, R.L., Friedrich, M., Grootes, P.M., Guilderson, T.P., Hajdas, I., Heaton, T.J., Hogg, A.G., Hughen, K.A., Kaiser, K.F., Kromer, B., McCormac, F.G., Manning, S.W., Reimer, R.W., Richards, D.A., Southon, J.R., Talamo, S., Turney, C.S.M., van der Plicht, J., Weyhenmeyer, C.E., 2009. IntCal09 and Marine09 radiocarbon age calibration curves, 0–50,000 years cal BP. *Radiocarbon* 51 (4), 1111–1150.
- Schnepp, E., Lanos, P., 2005. Archaeomagnetic secular variation in Germany during the past 2500 years. *Geophys. J. Int.* 163, 479–490.
- Schnepp, E., Lanos, P., 2006. A preliminary secular variation reference curve for archaeomagnetic dating in Austria. *Geophys. J. Int.* 166, 91–96.
- Stacey, F.D., 1967. The Koenigsberger ratio and the nature of thermoremanence in igneous rocks. *Earth Planet. Sci. Lett.* 2, 67–68.
- Straus, L.G., González Morales, M., 2003. El Mirón Cave and the 14C chronology of Cantabrian Spain. *Radiocarbon* 45, 41–58.
- Straus, L.G., González Morales, M., 2007. Further radiocarbon dates for the Upper Paleolithic of El Mirón Cave (Ramales de la Victoria, Cantabria, Spain). *Radiocarbon* 49, 1205–1214.
- Straus, L.G., González Morales, M., 2010. The radiocarbon chronology of el Mirón cave (Cantabria, Spain): new dates for the Initial Magdalenian occupations. *Radiocarbon* 52, 32–39.
- Straus, L.G., González Morales, M., 2012. El Mirón Cave. University of New Mexico Press, Albuquerque. 444 pp.
- Straus, L.G., González Morales, M., Farrand, W., Hubbard, W., 2001. Sedimentological and stratigraphic observations on El Mirón: a late Quaternary cave site in the Cantabrian Cordillera. *Geoarchaeology* 16, 603–630.
- Tema, E., Hedley, I., Lanos, Ph., 2006. Archaeomagnetism in Italy: a compilation of data including new results and a preliminary Italian secular variation curve. *Geophys. J. Int.* 167, 1160–1171.
- Tema, E., Kondopoulou, D., 2012. Secular variation of the Earth's magnetic field in the Balkan region during the last eight millennia based on archaeomagnetic data. *Geophys. J. Int.* 186, 603–614.
- Thébaud, E., Gallet, Y., 2010. A bootstrap algorithm for deriving the archeomagnetic field intensity variation curve in the Middle East over the past 4 millennia BC. *Geophys. Res. Lett.* 37, L22303, <http://dx.doi.org/10.1029/2010GL044788>.
- Vergés, J.M., 2011. La combustión del estiércol: aproximación experimental a la quema en montón de los residuos de redil. In: Morgado, A., Baena, J., García, D. (Eds.), *La investigación experimental aplicada a la Arqueología*. Universidad de Granada, pp. 325–330.
- Vergés, J.M., Allué, E., Angelucci, D., Burjachs, F., Carrancho, A., Cebrià, A., Expósito, I., Fontanals, M., Moral, S., Rodríguez, A., Vaquero, M., 2008. Los niveles neolíticos de la cueva de El Mirador (Sierra de Atapuerca, Burgos): nuevos datos sobre la implantación y el desarrollo de la economía agropecuaria en la submeseta norte. In: Hernández, M., Soler, J.A. (Eds.), *Actas del IV Congreso del Neolítico Peninsular*. Museo Arqueológico de Alicante, Alicante, Spain, pp. 418–427.
- Vergés, J.M., Allué, E., Angelucci, D.E., Cebrià, A., Díez, C., Fontanals, M., Manyanós, A., Montero, S., Moral, S., Vaquero, M., Zaragoza, J., 2002. La Sierra de Atapuerca durante el Holoceno: datos preliminares sobre las ocupaciones de la Edad del Bronce en la cueva de El Mirador (Ibeas de Juarros, Burgos). *Trab. Prehist.* 59 (1), 107–126.
- Zananiiri, I., Batt, C.M., Lanos, Ph., Tarling, D.H., Linford, P., 2007. Archaeomagnetic secular variation in the UK during the past 4000 years and its application to archaeomagnetic dating. *Phys. Earth Planet. Inter.* 160 (2), 97–107.